Assessment of the Several Structures Proposed for Tourmaline

By M. J. Buerger, Charles W. Burnham and Donald R. Peacor

Crystallographic Laboratory, Massachusetts Institute of Technology, Cambridge, Mass., U.S.A.

Different versions for the structure of tourmaline have been proposed by the Buerger, Ito and Belov schools. In order to settle the confused status of this important structure, an attempt was made to refine each model independently. For this purpose new intensity data were obtained from a crystal of the De Kalb, N.Y., material, which was ground to a small sphere in order to permit applying a simple and accurate correction for absorption. The intensities were measured with a single-crystal counter diffractometer. Starting with the coordinates for the several models, each was refined by least squares. The coordinates of the Buerger and Ito models converged to identical values, with $R(hkl) = 6 \cdot 9\%$.

In at least the tourmaline used for the intensity data, the Mg atoms occupy the central region of the octahedral sheet, and the tourmaline 'units' are knitted together by Al octahedra in spite of a great flexibility of replacement of octahedral sites. The alkali atom appears to be partly bonded to a girdle of saturated oxygen atoms which are part of the hexagonal ring of Si tetrahedra. This is reflected in an increase in the distances of these oxygen atoms from Si by $0 \cdot 03$ Å.

Introduction

Three more or less related structures have been proposed for tourmaline by Hamburger & Buerger (1948), Belov & Belova (1949, 1950) and Ito & Sadanaga (1951). Up to the present time no serious effort has been made to test the relative merits of these structures. As a result, the true structure of tourmaline is in doubt, and it has even been suggested that tourmaline is polymorphous (Donnay, Wyart & Sabatier, 1959), some tourmaline having the structure of the Buerger school, other tourmaline the structure of the Ito school. Since such confusion is intolerable, this investigation was instituted.

The Buerger and Ito structures are basically the same. They differ chiefly in minor variations of atomic coordinates which do not affect the fundamental bonding pattern. These structures are characterized by a hexagonal ring of Si tetrahedra which has the general shape of a hexagonal fragment isolated from a phyllosilicate sheet. The Mg atoms are in octahedral coordination and the octahedra share edges to form a trigonal fragment of a brucite-like layer. Six oxygen atoms of the lower part of this layer are also the apices of the hexagonal ring of Si tetrahedra. The trigonal nucleus of Mg octahedra is extended by six Al octahedra through edge sharing. Each of the B atoms is in triangular coordination, linked to the vertices of the octahedra of this layer.

The Belov structure does not have the same bonding pattern. It is based upon a double hexagonal ring of general formula $A_{12}O_{30}$, somewhat similar to the $Si_{12}O_{30}$ ring in milarite. In the Belov tourmaline structure, the tetrahedra of one ring contain 6 Si, the other a mixture of 3 Al + 3 B. These double rings are held together in columns along the c axis by Na
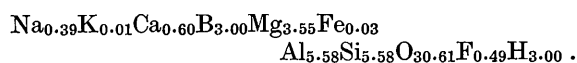
atoms, and the columns are bonded together by Mg atoms in octahedra which spiral up the 3-fold screw axis by sharing edges. The Buerger and Ito structures are based upon 31 oxygen atoms per cell; the Belov structure is based upon 30.

A necessary condition that a structure be essentially correct is that by minor adjustments of the coordinates of its atoms, the computed amplitudes can be brought into good agreement with the observed amplitudes. The three proposed structures of tourmaline can be subjected to this test, specifically by attempting to refine each by the method of least squares. To this end a set of excellent intensities is needed.

Experimental procedure

Entirely new intensity measurements were made using a single-crystal counter diffractometer (Buerger, 1960, p. 119). The intensities were gathered from tourmaline from de Kalb, New York. This was chosen because it is almost free of Fe, and because it has an otherwise comparatively simple composition. This material was taken from the same lot which was used by Hamburger & Buerger (1948) in their original determination.

The symmetry of tourmaline is $R3m$. New values for the edges of the hexagonal cell of the de Kalb tourmaline are $a = 15 \cdot 951 \pm 0 \cdot 001$, $c = 7 \cdot 24 \pm 0 \cdot 01$ Å. By combining the published chemical analyses, density and precision cell data, the composition of a primitive cell for this tourmaline can be expressed as

$$Na_{0 \cdot 39}K_{0 \cdot 01}Ca_{0 \cdot 60}B_{3 \cdot 00}Mg_{3 \cdot 55}Fe_{0 \cdot 03}$$
$$Al_{5 \cdot 58}Si_{5 \cdot 58}O_{30 \cdot 61}F_{0 \cdot 49}H_{3 \cdot 00} \, .$$

A number of crystal fragments were tested for perfection by examining their single-crystal diffraction

patterns, and the most perfect were ground into spheres and oriented. The one finally used for intensity measurement had a radius of $R = 0.00625$ cm. The linear absorption coefficient for this tourmaline is 103 cm.$^{-1}$, so that $\mu R = 0.644$.

The single-crystal diffractometer employed a Geiger tube as detector; strong reflections were reduced by aluminum absorbers so that the linearity range was not exceeded. Any errors in calibrating the absorbers were minimized by the use of different scale factors for reflections measured under different absorber conditions. The intensities were measured by digital counting, due allowance being made for background on both sides of a peak. There are about 440 reflections in the asymmetric unit within the accessible sphere. Of these, 375 were within the recording range of the apparatus, and their intensities were measured with copper radiation. They were corrected for Lorentz, polarization and absorption factors.

Refinement of the Buerger and Ito structures

The Buerger and Ito structures, while very similar, are described by their authors in different ways. To transform either to the other, it is necessary to rotate it through π about the a_3 axis of the hexagonal cell and displace it parallel to c. In transforming coordinates from one to the other, therefore, it is necessary to interchange x and y, reverse the sign of z, and then add a constant to z. We have arbitrarily chosen to transform the Buerger to the Ito coordinates for purposes of comparing the structures. The original coordinates of Al and O$_8$ of the Buerger structure were transformed by symmetry operations in such a way that all coordinates now refer to atoms within a small asymmetric unit bounded by adjacent mirrors and intersecting in a screw axis (see Fig. 3, beyond). This places all atoms in the same cell and as near as possible to the 3-fold axis through the origin.

Since the origin along the c axis is not symmetry fixed, it can be chosen arbitrarily. The same origin was chosen for all three structures by keeping the z coordinates of Si constant throughout the refinements. The initial coordinates of the Ito structure and the transformed coordinates of the Buerger structure are listed in Tables 1 and 2 for comparison.

The composition of the de Kalb tourmaline, noted in an earlier section, fits neatly into the Buerger and Ito structures according to the following scheme:

Central void	Tri-angular	Octa-hedral	Octa-hedral	Tetra-hedral		
Na$_{0.39}$			Al$_{5.42}$	Si$_{5.84}$	O$_{30.61}$	H$_{3.00}$
K$_{0.01}$	B$_{3.00}$	Mg$_{3.00}$	Mg$_{0.55}$	Al$_{0.16}$	F$_{0.47}$	
Ca$_{0.60}$			Fe$_{0.03}$			
1.00			6.00	6.00	31.08	

Table 1. Results of refining the Ito tourmaline structure
(Old coordinates above, new below: Buerger designation left, Ito right)

Equi-point	Atom	x	$\sigma(x)$	y	$\sigma(y)$	z	$\sigma(z)$	B
3a	Na, Ca	0		0		0.961		
		0	—	0	—	0.8576	0.0010	0.688
	O$_1$ = OH$_2$	0		0		0.331		
		0	—	0	—	0.3117	0.0022	−0.678
9b	O$_2$ = O$_V$	0.110		0.055		0.621		
		0.1218	0.0010	0.0609	0.0005	0.6113	0.0013	0.378
	O$_4$ = O$_{II}$	0.188		0.094		0.011		
		0.1870	0.0010	0.0935	0.0005	0.0176	0.0014	0.526
	B	0.208		0.104		0.641		
		0.2206	0.0015	0.1103	0.0007	0.6362	0.0020	−0.228
	Mg = Li, Al	0.063		0.125		0.471		
		0.0635	0.0002	0.1270	0.0005	0.4618	0.0007	0.327
	O$_5$ = O$_{III}$	0.094		0.188		0.011		
		0.0906	0.0005	0.1812	0.0010	0.0012	0.0012	−0.040
	O$_3$ = OH$_{II}$	0.125		0.250		0.621		
		0.1340	0.0005	0.2680	0.0010	0.5755	0.0014	0.548
18c	Si	0.188		0.188		0.090		
		0.1898	0.0003	0.1922	0.0003	0.0900	fixed z	0.201
	Al	0.270		0.297		0.491		
		0.2615	0.0003	0.2976	0.0003	0.4762	0.0006	0.167
	O$_7$ = O$_I$	0.280		0.280		0.011		
		0.2851	0.0006	0.2844	0.0007	0.0090	0.0010	0.301
	O$_6$ = O$_{IV}$	0.188		0.188		0.331		
		0.1866	0.0007	0.1952	0.0006	0.3111	0.0009	0.178
	O$_8$ = O$_{VI}$	0.261		0.210		0.651		
		0.2698	0.0007	0.2085	0.0007	0.6455	0.0011	0.694

Table 2. *Results of refining the Buerger tourmaline structure*

(Old coordinates above, new below: Buerger designations left, Ito right)

Equi-point	Atom	x	$\sigma(x)$	y	$\sigma(y)$	z	$\sigma(z)$	B
3a	Na, Ca	0		0		0·826		
		0	—	0	—	0·8576	0·0010	0·688
	$O_1 = OH_I$	0		0		0·297		
		0	—	0	—	0·3117	0·0022	−0·678
9b	$O_2 = O_V$	0·116		0·058		0·612		
		0·1218	0·0010	0·0609	0·0005	0·6113	0·0013	0·378
	$O_4 = O_{II}$	0·192		0·096		0·019		
		0·1870	0·0010	0·0935	0·0005	0·0176	0·0014	0·526
	B	0·234		0·117		0·612		
		0·2206	0·0015	0·1103	0·0008	0·6362	0·0020	−0·229
	$Mg = Li, Al$	0·067		0·134		0·458		
		0·0635	0·0002	0·1270	0·0004	0·4618	0·0007	0·327
	$O_5 = O_{III}$	0·080		0·160		0·090		
		0·0906	0·0004	0·1812	0·0008	0·0012	0·0012	−0·040
	$O_3 = OH_{II}$	0·117		0·234		0·674		
		0·1340	0·0005	0·2680	0·0010	0·5755	0·0014	0·548
18c	Si	0·192		0·192		0·090		
		0·1898	0·0003	0·1922	0·0003	0·0900	fixed z	0·201
	Al	0·269		0·302		0·445		
		0·2615	0·0003	0·2976	0·0003	0·4762	0·0006	0·167
	$O_7 = O_I$	0·255		0·275		−0·059		
		0·2851	0·0006	0·2844	0·0007	0·0090	0·0010	0·301
	$O_6 = O_{IV}$	0·196		0·196		0·297		
		0·1866	0·0007	0·1952	0·0006	0·3111	0·0009	0·178
	$O_8 = O_{VI}$	0·286		0·236		0·612		
		0·2698	0·0007	0·2085	0·0007	0·6455	0·0011	0·694

The composition of the cell evidently requires 31 oxygen atoms.

For refinement purposes, the atomic scattering factor for each atom site was computed from the appropriate average of the half-ionized atoms in the formula for that site. Refinement of the structures was started with reasonable individual isotropic temperature factors, namely,

$$B_{Si} = B_{Al} = B_{Mg} = B_B = 0·2; \quad B_O = 0·4; \quad B_{Na} = 0·5 .$$

Before refining the Ito structure, its value of R was 31%. After two cycles of least-squares refinement, the R was 26%. Since this value of R appeared rather high, it seemed wise to check the structure for possible gross errors in atom location. Accordingly a three-dimensional Fourier synthesis $\varrho(xyz)$, based upon the coordinates resulting from the second cycle, was prepared. This showed that all atoms were in approximately their correct locations except for Na and OH_I. The peak shapes for these atoms required fairly large adjustments in z.

After making this adjustment, the structure was refined by 18 more least-squares cycles using the Busing & Levy (1960) program for the IBM 704 computer. Cycles 3 through 7 reduced $R(hkl)$ to 8·3%. From this point on, the fixed temperature factors were replaced by variable isotropic temperature factors,

except in cycles 11, and 14 through 18, in which temperature factors were held constant and coordinates and scale factors alone allowed to vary. During the cycles in the middle of the sequence anisotropic temperature factors were used, but these did not improve R, and the final cycles were made with individual but isotropic temperature factors. The final value of $R(hkl)$ for 20 cycles was 6·9%. The initial and final coordinates, along with their standard deviations, are given in Table 1.

The initial value of R for the Buerger structure was 35%. Ten cycles of least-squares refinement reduced R to 21%. At this point a three-dimensional difference synthesis, $\varDelta\varrho(xyz)$, was computed; this showed comparatively random background except in the neighborhood of O_5 and O_3 where anomalies calling for obvious displacement were noted. When these coordinate changes were made, the R was immediately improved to 11·6%, and after two more cycles was reduced to 6·9%. After 3 more cycles with arbitrary B's, and 7 more with variable isotropic B's (in certain of which the B's previously found were fixed but coordinates and scale factors alone allowed to vary) the refinement had converged, although the final value of $R(hkl)$ was still 6·9%.

The initial and final coordinates, along with their standard deviations, are given in Table 2. The final coordinates, with their standard deviations, and the

refined values of the isotropic temperature factors, are identical with those of Table 1, obtained in the refinement of the Ito structure.

The final set of temperature factors contains three having negative values, namely those for B, O_1 and O_5. Another cycle of refinement was run with the boron treated as un-ionized and these oxygens as fully ionized. This had an almost unappreciable effect on the coordinates and temperature factors.

Attempt to refine the Belov structure

The Belov structure has the same general placement of oxygen atoms as the Buerger structure except that, as noted, there is an additional oxygen atom in the Buerger structure (which is required to provide the common oxygen atom of the three Mg octahedra in

the central part of the layer). Indeed, oxygen atoms of the Belov structure have been labelled the same as oxygen atoms of similar coordinates in the Buerger structure, except for a small difference in the arbitrary origin of z. It may accordingly be assumed that the Belov structure was derived from the Buerger structure by utilizing nearly the same oxygen set and displacing the metals of the BO_3 triangles and Mg octahedra layer so that they occupy tetrahedral voids between oxygens. (In addition, the Mg and Al are also interchanged.)

Because of this similarity, it is convenient to transform the Belov structure to the Ito orientation in order to compare the course of the refinements. In effect this brings the Si layer into correspondence in all three structures.

Table 3. *Belov's structure for tourmaline before and after refinement*
(Ito's orientation)

Equi-point	Atom	x	$\sigma(x)$	y	$\sigma(y)$	z	$\sigma(z)$
3a	Na	0		0		0·839	
		0	—	0	—	0·8537	0·0041
9b	O_{II}	0·107		0·054		0·579	
		0·1260	0·0040	0·0630	0·0020	0·6212	0·0055
	O_{III}	0·122		0·243		0·629	
		0·1382	0·0022	0·2764	0·0044	0·5889	0·0059
	O_{IV}	0·073		0·146		0·004	
		0·0915	0·0022	0·1830	0·0044	−0·0058	0·0054
	O_V	0·204		0·102		−0·011	
		0·1836	0·0044	0·0918	0·0022	0·0216	0·0053
18c	Mg	0·056		0·314		0·494	
		0·0369	0·0013	0·2962	0·0013	0·4859	0·0026
	(B+Al)	0·158		0·176		0·524	
		0·1559	0·0019	0·1735	0·0019	0·4865	0·0031
	Si	0·192		0·192		0·090	
		0·1899	0·0011	0·1914	0·0011	0·090	(fixed z)
	O_{VI}	0·182		0·183		0·309	
		0·1860	0·0030	0·1898	0·0031	0·3162	0·0038
	O_{VII}	0·283		0·297		0·019	
		0·2807	0·0028	0·2849	0·0029	0·0065	0·0045
	O_{VIII}	0·260		0·050		0·634	
		0·2736	0·0029	0·0638	0·0030	0·6450	0·0042

Table 4. *Coordinates of the refined tourmaline structure*

Equi-point	Atom	x	$\sigma(x)$	y	$\sigma(y)$	z	$\sigma(z)$	B
3a	Na	0	—	0	—	0·8576	0·0010	0·688
	$O_1 = OH_I$	0	—	0	—	0·3117	0·0022	−0·678
9b	$O_2 = O_V$	0·1218	0·0010	0·0609	0·0005	0·6113	0·0013	0·378
	$O_4 = O_{II}$	0·1870	0·0010	0·0935	0·0005	0·0176	0·0014	0·526
	B	0·2206	0·0015	0·1103	0·0008	0·6362	0·0020	−0·229
	Mg = Li, Al	0·0635	0·0005	0·1270	0·0005	0·4618	0·0007	0·327
	$O_5 = O_{III}$	0·0906	0·0005	0·1812	0·0010	0·0012	0·0012	−0·040
	$O_3 = OH_{II}$	0·1340	0·0005	0·2680	0·0010	0·5755	0·0014	0·548
18c	Si	0·1898	0·0003	0·1922	0·0003	0·0900	—	0·201
	Al	0·2615	0·0003	0·2976	0·0003	0·4762	0·0006	0·167
	$O_7 = O_I$	0·2851	0·0006	0·2844	0·0007	0·0090	0·0010	0·301
	$O_6 = O_{IV}$	0·1866	0·0007	0·1952	0·0006	0·3111	0·0009	0·178
	$O_8 = O_{VI}$	0·2698	0·0007	0·2085	0·0007	0·6455	0·0011	0·694

Although the analysis of the de Kalb tourmaline provides about 3 Mg, 3 B and 6 Al atoms, Belov's structure requires (3 Al + 3 B) and 6 Mg. Accordingly, as much Mg as possible was placed in the octahedra, the remainder being made up by Al. The atoms of the cell, noted previously, were accordingly distributed as follows:

Central void	Octa-hedral	Tetra-hedral	Tetra-hedral	
$Na_{0.39}$	$Mg_{3.55}$	$B_{3.00}$	$Si_{5.89}$	
$K_{0.01}$	$Fe_{0.03}$	$Al_{3.00}$	$Al_{0.16}$	O_{30}
$Ca_{0.60}$	$Al_{2.42}$			
1.00	6.00	6.00	6.00	

The additional $O_{0.61} + F_{0.47}$ indicated by the analysis was necessarily ignored.

For the purposes of the refinement, the atomic scattering factor for each atom site was computed from the appropriate average of the half-ionized atoms in that site according to the distribution in the formula just given. Isotropic temperature factors appropriate to the sites ($B_{Si} = B_{Al} = B_{Mg} = 0.2$; $B_O = 0.4$; $B_{Na} = 0.5$) were applied, and were fixed during the refinement of coordinates and scale factors. The
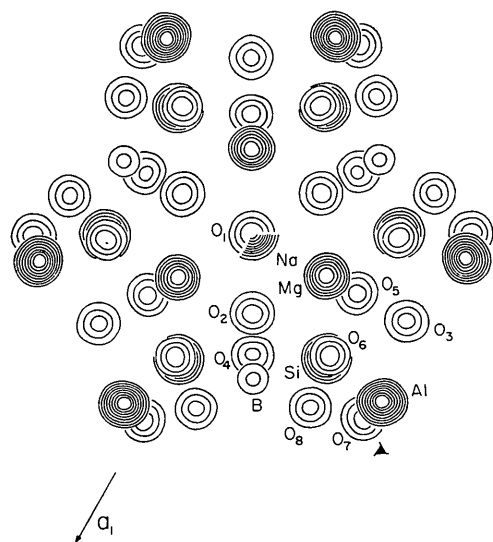
Fig. 1. Projection of the maxima of $\varrho(xyz)$ on (0001) of the hexagonal unit cell. (Contour interval 5 e.Å^{-3}.)

Fig. 2. Interpretation of Fig. 1. (a) The lower layer of the structure comprising a ring of six rather regular Si tetrahedra.

(b) The upper layer of the structure chiefly consisting of octahedra. The central three larger octahedra contain Mg. The six smaller peripheral octahedra contain Al. The small circles are B atoms bonded along the broken lines to the corners of octahedra. The lower right octahedron is pierced by a 3_1 screw axis to provide correlation with Fig. 2(c).

(c) The manner in which the various octahedral layers of the structure are joined to each other. The specific octahedron mentioned in the legend of Fig. 2(b) is seen here to share an edge with its 3_1 screw equivalent below it. Other features of the structure are omitted to focus attention on the nature of the bonding between these octahedra.
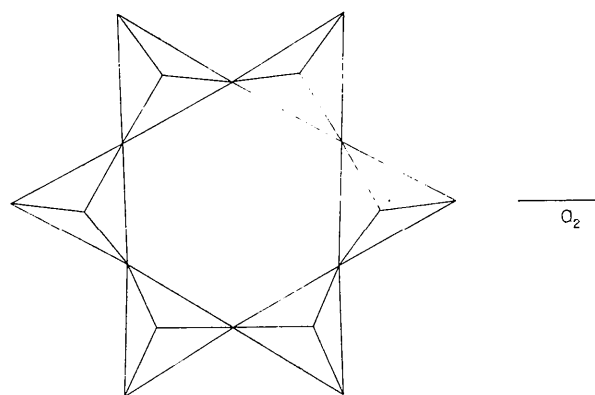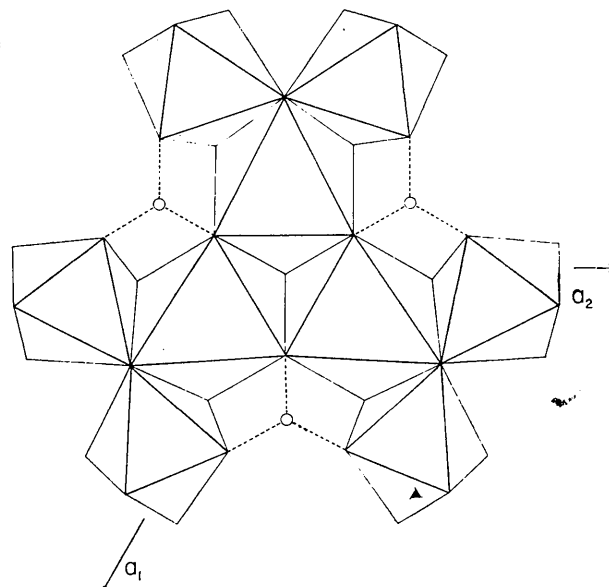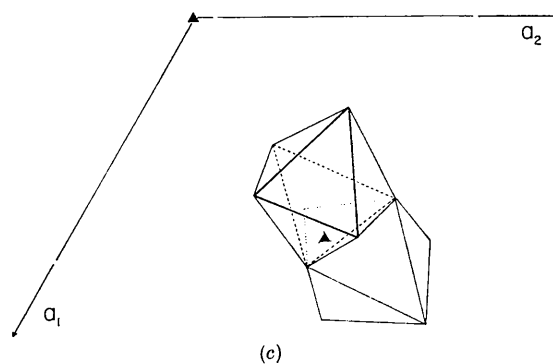
least-squares refinement substantially converged after 7 cycles. The initial and final results are given in Table 3. For the final structure, $R = \Sigma ||F_o| - |F_c||/\Sigma|F_o|$ has the high value of 27·9%, so the structure can hardly be correct.

To study the state of the structure at this point, a three-dimensional difference synthesis, $\Delta\varrho(xyz)$, was computed and then plotted in sections parallel to (0001). These maps were characterized by a random topography having maximum heights and depths in the neighborhood of 2 e.Å^{-2}. Most of the atom locations fell on moderate gradients. The site for B+Al, however, fell at the location of a conspicuous minimum with a $\Delta\varrho$ of 9 e.Å^{-2}. This negative anomaly was near two maxima on symmetry planes, one having the modest height of 2 e.Å^{-2}, the other of height 13 e.Å^{-2}, making it the most conspicuous feature on any of the maps. If the B and Al atoms of the B+Al site are redistributed to the locations of these positive anomalies, the result is a structure which bears a resemblance to the Buerger and Ito structures (except that the Al and Mg are interchanged and that the oxygen atom on the 3-fold axis is missing). Without this redistribution the Belov structure cannot be refined, and must be considered as incorrect.

Characteristics of the tourmaline structure

The coordinates of the final tourmaline structure are given in Table 4. To illustrate the relations between atoms in this important structure, a three-dimensional Fourier synthesis was prepared based upon structure factors computed from a near-final set of coordinates. This has the characteristics of a well refined structure, with well rounded contours and slightly undulating, random background. The sections of this synthesis containing the peak values of $\varrho(xyz)$ are shown projected on (0001) in Fig. 1. In Figs. 2(a), (b), and (c) this projection is interpreted. Fig. 2(a) shows the hexagonal ring of Si tetrahedra lying at the lowest level of the structure. This is seen to have a fairly regular hexagonal form (a feature which the original Ito structure possessed). Fig. 2(b) shows the next higher layer of the structure, a sheet of octahedra. The central three octahedra are occupied by Mg, an identification confirmed by their larger size. The pairs of octahedra on the edges are occupied by Al, an identification confirmed by their smaller size. Thus in spite of the great flexibility in the replacement of the metals of the octahedral sites in tourmaline, the Mg and Al atoms appear to play distinct roles. Three B atoms help bind together the octahedral layer.

A 3_1 screw is shown piercing the lower right Al octahedron of Fig. 2(b). (Since all Al's are equivalent, a corresponding 3_1 or 3_2 screw pierces each Al octahedron.) This particular octahedron and its screw symbol are repeated in Fig. 2(c), an illustration which is intended to show how layers such as shown in Fig. 2(b) are linked in depth. For clarity, Fig. 2(c)

shows only one Al octahedron and its 3_1 screw equivalent at a level $\frac{1}{3}$ lower; each pair of screw-equivalent Al octahedra share a common edge. If the third Al octahedron related by the 3_1 screw in Fig. 2(c) were shown, it would complete a set of three Al octahedra related by and spiraling down the 3_1 axis.

The alkali atom fits in the central void of the ring of tetrahedra in Fig. 2(a), just below the level of the base of the ring. Directly above the alkali, and in the center of Fig. 2(b), is the hydroxyl, O_1, and just below the alkali atom are the three O_2's in the triangle immediately surrounding that hydroxyl, also in Fig. 2(b).
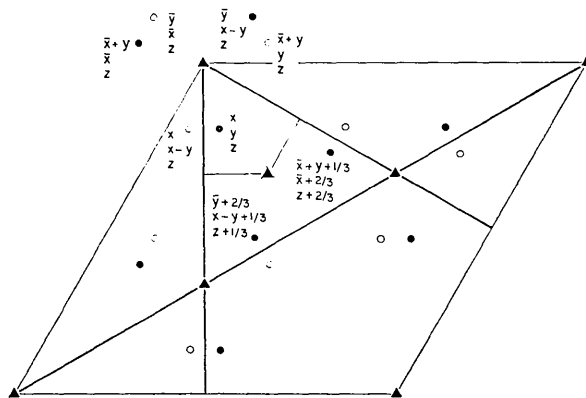

Fig. 3. Some of the symmetry elements in a hexagonal cell of $R3m$ and some of the equivalent positions and their coordinates which are helpful in understanding the atom locations used in Table 5. The asymmetric unit can be taken as either: (1) the content of the trigonal prism of height $c/3$ and whose sides are three mirrors, or (2) the content of the four-sided prism of height c whose sides are two mirrors plus two perpendicular planes dropped to these from the screw axis. This asymmetric unit is utilized in this paper.

The structure can be studied in more detail with the aid of the interatomic distances shown in Table 5. The coordinates of certain equivalent points of space group $R3m$ are shown in Fig. 3 as an aid to the interpretation of the entries in Table 5.

The Na(Ca) atom has ten near neighbors. The closest are the three O_2's at 2·46 Å, which is consistent with the sum of the radii of calcium and oxygen ions. Curiously, the next six nearest neighbors are the six saturated oxygen atoms of the tetrahedral ring, namely three O_5 at 2·73 Å and three O_4 at 2·83 Å. The unsaturated hydroxyl O_1, is at the comparatively great distance of 3·29 Å.

In the tetrahedral ring, the Si atom is at equal distances, 1·603 and 1·606 Å, from two oxygens (O_6 and O_7) which are not near to Na, but at greater though almost equal distances, 1·635 and 1·639 Å, from the oxygens (O_5 and O_4) which are near Na. This difference, namely 0·03 Å, in Si–O distances in the same tetrahedron suggests weak bonds from Na to O_5 and O_4 of the ring of silica tetrahedra, and correspondingly weakened Si–O bonds.

Table 5. *Important interatomic distances in the refined tourmaline structure*

Silicon coordination polyhedron

				s	$\sigma(s)$
Si	x, y, z	O_4	$x, y\ z$	1·639 Å	0·003 Å
		O_5	x, y, z	1·635	0·003
		O_6	x, y, z	1·603	0·007
		O_7	x, y, z	1·606	0·009
O_6	x, y, z	O_4	x, y, z	2·675	0·008
		O_5	x, y, z	2·662	0·007
		O_7	x, y, z	2·654	0·010
O_4	x, y, z	O_5	x, y, z	2·547	0·006
		O_7	x, y, z	2·638	0·009
O_5	x, y, z	O_7	x, y, z	2·689	0·009

Magnesium octahedron

					s	$\sigma(s)$
Mg	x, y, z		O_1	x, y, z	2·063 Å	0·026 Å
		(2)	O_2	x, y, z	2·032	0·010
		(2)	O_6	x, y, z	2·023	0·009
			O_3	x, y, z	2·116	0·011
O_1	x, y, z	(2)	O_2	x, y, z	2·746	0·019
		(2)	O_6	x, y, z	3·047	0·021
O_3	x, y, z	(2)	O_6	x, y, z	2·587	0·008
		(2)	O_2	x, y, z	3·222	0·011
O_2	x, y, z		O_2''	$x+y, y, z$	2·916	0·011
			O_6	x, y, z	2·857	0·008
O_6	x, y, z		O_6''	$x+y, y, z$	2·846	0·019

Aluminum octahedron

				s	$\sigma(s)$
Al	x, y, z	O_3	x, y, z	1·979 Å	0·004 Å
		O_6	x, y, z	1·890	0·009
		O_8	x, y, z	1·930	0·010
		O_{7*}	$\bar{y}+\frac{2}{3}, x-y+\frac{1}{3}, z+\frac{1}{3}$	1·966	0·010
		O_{7**}	$\bar{x}+y+\frac{1}{3}, \bar{x}+\frac{2}{3}, z+\frac{2}{3}$	1·910	0·009
		O_{8-*}	$\bar{x}+y+\frac{1}{3}, \bar{x}+\frac{2}{3}, z-\frac{1}{3}$	1·919	0·010
O_3	x, y, z	O_6	x, y, z	2·587	0·008
		O_8	x, y, z	2·812	0·011
		O_{7**}	$\bar{x}+y+\frac{1}{3}, \bar{x}+\frac{2}{3}, z+\frac{2}{3}$	2·847	0·009
		O_{8-*}	$\bar{x}+y+\frac{1}{3}, \bar{x}+\frac{2}{3}, z-\frac{1}{3}$	2·860	0·010
O_7	$\bar{y}+\frac{2}{3}, x-y+\frac{1}{3}, z+\frac{1}{3}$	O_6	x, y, z	2·790	0·014
		O_8	x, y, z	2·907	0·012
		O_{7**}	$\bar{x}+y+\frac{1}{3}, \bar{x}+\frac{2}{3}, z+\frac{2}{3}$	2·762	0·008
		O_{8-*}	$\bar{x}+y+\frac{1}{3}, \bar{x}+\frac{2}{3}, z-\frac{1}{3}$	2·431	0·013
O_6	x, y, z	O_8	x, y, z	2·717	0·010
		O_{8-*}	$\bar{x}+y+\frac{1}{3}, \bar{x}+\frac{2}{3}, z-\frac{1}{3}$	2·797	0·013
O_7	$\bar{x}+y+\frac{1}{3}, \bar{x}+\frac{2}{3}, z+\frac{2}{3}$	O_{8-*}	$\bar{x}+y+\frac{1}{3}, \bar{x}+\frac{2}{3}, z-\frac{1}{3}$	2·856	0·010
		O_8	x, y, z	2·431	0·014

Boron triangle

					s	$\sigma(s)$
B	x, y, z		O_2	x, y, z	1·375 Å	0·010 Å
		(2)	O_8	x, y, z	1·358	0·010
O_8	x, y, z	(2)	O_2	x, y, z	2·369	0·010
			O_8'	$x, x-y, z$	2·348	0·021

Sodium coordination polyhedron

					s	$\sigma(s)$
Na	x, y, z	(3)	O_2	x, y, z	2·452 Å	0·005 Å
Na	$x, y, z-1$		O_1	x, y, z	3·288	0·007
		(3)	O_4	x, y, z	2·831	0·003
		(3)	O_5	x, y, z	2·711	0·003

The obvious difference in size between the central and peripheral octahedra of Fig. 2(b) is borne out by their computed metal–oxygen distances. The central octahedra have about 2·05 Å, which compares reasonably well with the Mg octahedra in enstatite (2·19 Å) and protoenstatite (2·12 Å). The mean metal–oxygen distances in the peripheral octahedra are 1·93 Å, in exact agreement with the mean for the Al octahedra of andalusite (Burnham & Buerger, 1961).

The edges shared between Al octahedra are 2·43 Å, which compares well with 2·47 Å, the shared edges in andalusite. The edge of the Mg octahedron shared with another Mg octahedron (O_1O_2) is shortened to 2·75 Å; the edge shared with the Al octahedron (O_3O_6) is considerably shorter, 2·58 Å. This feature is expectable because of the larger charge on the Al ion and its smaller radius.

References

BELOV, N. V. & BELOVA, E. N. (1949). *Dokl. Akad. Nauk S.S.S.R.* **69**, 185. (Abstracted in *Phys. Abstr.* **53**, (1950) item 3545).

BELOV, N. V. & BELOVA, E. N. (1950). *Dokl. Akad. Nauk S.S.S.R.* **75**, 807.

BUERGER, M. J. (1960). *Crystal-structure Analysis*, p. 118. New York: Wiley.

BURNHAM, C. W. & BUERGER, M. J. (1961). *Z. Kristallogr.* **115**, 269.

BUSING, W. R. & LEVY, H. A. (1959). *A crystallographic least-squares refinement program for the IBM 704.* Oak Ridge, Tennessee. Oak Ridge National Laboratories.

DONNAY, GABRIELLE & BUERGER, M. J. (1950). *Acta Cryst.* **3**, 379.

DONNAY, GABRIELLE, WYART, J. & SABATIER, G. (1959). *Z. Kristallogr.* **112**, 161.

HAMBURGER, GABRIELLE E. & BUERGER, M. J. (1948). *Amer. Min.* **33**, 532.

ITO, T. & SADANAGA, R. (1951). *Acta Cryst.* **4**, 385.

Résolution des Structures Cristallines: Méthode des »Domaines Interdits«

PAR GÉRARD VON ELLER

Laboratoire de Rayons X de l'IRChA, 12, quai Henri IV, Paris IVe, France

The notion of inequality between structure factors has been extended. This leads to associate a Fourier series with each Karle–Hauptman matrix U. The amplitudes and phases of this real positive series, $\varphi(\mathbf{x})$, (where $\mathbf{x}$ is the point of the unit cell) are the moduli and arguments of the elements of the matrix U^{-1} to which are attached the cristallographic indices of the corresponding elements of U. Wherever $\varphi(\mathbf{x})$ is greater than $1/n_j$ (n_j being the relative weight of the j atom), there is no atom of the j kind present.

1. Introduction

L'examen des déterminants de Karle & Hauptman (1950), ou, de façon équivalente, de l'espace des facteurs de structure (v. Eller, 1955, 1960, 1961), permet d'éliminer les combinaisons de phases $\alpha(\mathbf{h})$ incompatibles avec une répartition de densité électronique positive dans la maille cristalline. De la sorte toutes autres informations, portant par exemple sur la nature des atomes, leur nombre ou sur des données de configuration moléculaire, qui permettraient d'accélérer considérablement l'amorce de la résolution de la structure, restent malheureusement inemployées.

Il a donc paru intéressant de rechercher une voie qui permette de les utiliser. Elle a été trouvée dans une étude plus approfondie des formes hermitiques de Karle & Hauptman ainsi que dans l'interprétation de leurs transformées de Fourier dans l'espace cristallin, et impose l'optique suivante:

Pour une inégalité insatisfaite (déterminant de Karle & Hauptman négatif ou espace des facteurs de structure inconstructible), *il n'y a aucune place dans la maille pour des atomes.*

Pour une inégalité 'inconfortablement' satisfaite, *il n'y a pas de place pour des atomes dans certains domaines de la maille.*

Ces 'domaines interdits' peuvent être déterminés pour chaque application de phases aux $U(\mathbf{h})$ de toute matrice de Karle & Hauptman. Il devient alors possible d'éliminer celles de ces applications qui sont stériquement incompatibles avec les renseignements que l'on possède sur la configuration du motif cristallin.

2. Théorie

Soit dans une maille cristalline, sans symétrie pour plus de généralité, déformée suivant un cube de volume un pour simplifier le traitement mathéma-